Dose Calculation in a Mouse Lung Tumor and in Secondary Organs During Radiotherapy Treatment: A Monte Carlo Study

Mahdjoub Hamdi[1], Malika Mimi[1], and M'hamed Bentourkia[2,*]

[1] Department of Electrical Engineering, University of Mostaganem, Algeria
[2] Department of Nuclear Medicine and Radiobiology, Université de Sherbrooke, Canada
mhamed.bentourkia@usherbrooke.ca

Abstract. Radiotherapy in cancer treatment always affects surrounding tissues and even deposits doses in distant tissues not traversed by the radiation beams. In the present work, we report energy transfer and absorbed dose in a target tumor and in other distant organs in a digital mouse by Monte Carlo simulations. We simulated a selection of X-rays beams with seven energies, 50, 100, 150, 200, 250, 350 and 450 keV each oriented in seven irregularly incremented angles, and we computed the dose and the energy deposit as a function of photon interaction types. The results show that the absorbed dose increased with increasing energy even in the secondary organs not receiving the radiation beam, and that the lowest dose was obtained with 100 keV beam. The spinal cord, of comparable size to the tumor and excluding the spinal bones, which was not directly irradiated by the beams, received a dose representing in average 1% of that of the tumor, while the spinal bone received doses of 6.6 and 0.12 times those in the tumor at 50 and 450 keV, respectively. Such Monte Carlo simulations could be necessary to select the appropriate beam energy and beam angles to efficiently treat the tumor and to moderately reduce the impact of the radiations in the other organs.

Keywords: Dosimetry, Monte Carlo, Small animal, Tumor, X-rays, Photon interaction.

1 Introduction

With Intensity Modulated Radiation Therapy (IMRT), the external beam is adjusted in intensity and cross section to target the malignant tumor while preserving the normal tissues. The provided 3D anatomical images of structures with Computed Tomography (CT) serve as a guide for the radiation oncologist to precisely adjust the beam on the tumor and to select other beam trajectories. The beam flux, intensity, energy and orientation are then estimated to optimize the penetration of the beam until the target tissue. Monte Carlo simulations (MCS) are generally used to calculate dose distributions. MCS are accepted as the most accurate method for dose calculation, but

* Corresponding author.

F. Ortuño and I. Rojas (Eds.): IWBBIO 2015, Part I, LNCS 9043, pp. 360–367, 2015.

simulating a large number of particles and tracking their interactions in the medium need high memory and fast clusters of computers in conjunction with improved algorithms [1, 2].

Experimental preclinical small animal digital models are used to investigate tumor response to radiation therapy, and they are generally created from high resolution anatomical imaging such as magnetic resonance imaging, CT or from digital atlases [3-5].

The aims of the present work were to assess the radiotherapy dose deposit in a primary tumor and in other secondary organs of a mouse phantom [3] using multiple beam angles and energies targeting the tumor. To achieve these calculations we used Geant4 Applications for Tomographic Emission (GATE) based on Monte Carlo simulation code [6]. We also report the statistics of the transferred energy in the tumor and in the other tissues.

2 Materials and Methods

2.1 Heterogeneous Mouse Phantom

We used a digimouse based 3D image of a 28 g normal nude male mouse in format of micro-CT image provided by Digimouse [3] as shown in Fig. 1. Since the Digimouse data were obtained as gray scale intensities, we converted them to a voxelized phantom with density in Hounsfield Units (HU) [7, 8]. In fact, GATE utilizes HU, and within GATE, they are converted to mass densities. To convert mouse image from gray scale levels to HU, we chose two extreme volumes of interest (VOI) in air and in spinal bone in order to define the linearity between image intensities and tissues densities [7, 9, 10]. We evaluated the mean intensity values of each region as 0 for air and 254 for spinal bone, and we established their corresponding densities of 0.120×10^{-2} g/cm^3 and 1.85 g/cm^3, respectively. For calculation of HU values, we extracted the mass attenuation coefficients for these two materials from the tables of Photon Cross Sections and Attenuation Coefficients (http://atom.kaeri.re.kr/cgi-bin/w3xcom, the densities of the media are also given therein) by supposing 30 keV mono-energetic photon beam [3].

In the mouse phantom, we considered a lung tumor having 60 HU [11] with a spherical volume of 1.4 mm in diameter [12] (Fig. 1). The mean HU difference between the tumor and lung tissue was 625 HU. AMIDE Software [13] was used for image display and manipulation. For dosimetry analyses, we used 7 radiation beams focusing on the tumor and we evaluated photon interactions, energy transfer and the related absorbed dose in 8 volume regions including the tumor (Fig. 1). Volume 1 (V1) was around the tumor, V2 was in lung tissue, V3 was in lung tissue intercepted by beam 1, V4 and V5 were in the heart, V6 was located in the lung at the level of the tumor but horizontally translated by 1.8 mm, V7 was manually drawn around the spinal bone including bone marrow and spinal cord, and V8 was located around the spinal cord excluding the bone. The volumes of V7 in the spine and V8 in the spinal cord were respectively 7.32 and 1.09 times greater than the tumor volume (V1). In addition to the actual volume of the tumor, i.e. 1.4 mm of diameter (Fig. 1), the tumor volume was defined by two other regions of different diameters to assess the energy

transfer and absorbed dose within the beams and at larger volumes than intercepted by the beams, at diameters of 1.6 mm, V9, and 1.8 mm, V10. These assessments were made to estimate the dose to the boundaries of the tumor and to nearest tissues as the real limits of the tumor are not always accurately known from the images in clinical situations. All these regions were identified by means of the indications on the Digimouse atlas [3] (http://neuroimage.usc.edu/neuro/Digimouse_Download).

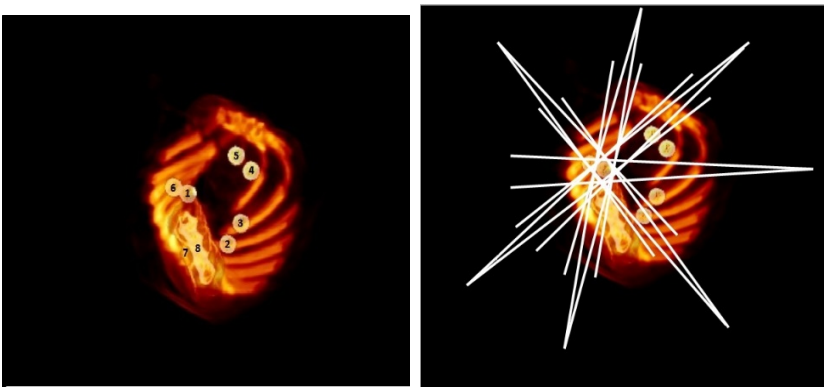

Fig. 1. Left: Mouse phantom with 8 tissue regions with region 1 being the targeted tumor. The circles around the digits indicate the actual spherical shape of the regions with 1.4 mm in diameter except for regions 7 and 8 which were manually drawn. Right: Same image repeated with 7 radiotherapy beams focused on the tumor only.

2.2 Simulation Procedure

A monoenergetic conical X-rays beam was simulated from a point source intercepting the tumor. Seven beams were used around the mouse phantom at 7 angles to avoid irradiating bone marrow and the spinal cord [14] (Fig. 1). To investigate the influence of the X-rays energies on the absorbed dose within the tumor, in its surrounding tissues and in the neighboring organs, the X-rays beams spanned the following energies of 50, 100, 150, 200, 250, 350 and 450 KeV with a total of $7x10^8$ photons simulated for each beam angle and energy. This number of photons corresponds to the expected absorbed dose, around 2 Gy, in a small volume of a mouse tissue, using 8 beams with a current of 50 mAs at 120 kVp [15, 16]. The simulations were conducted on a supercomputer having 2464 CPUs and 308 SGI XE320 compute nodes each with 2 Intel Xeon E5462 four core processors at 2.8 GHz and 16 to 32 Gbytes of memory per node (http://www.calculquebec.ca/en/resources/compute-servers/mammouth-serie-ii). A single beam with $7x10^8$ photons simulated in the mouse took around 5 min, and the whole beams for a single simulated energy were distributed on 40 nodes.

The radiation dose was calculated in each volume of the ten regions (Fig. 1). Also we concentrated our efforts here on energy transfer and absorbed dose in specific volume regions instead of lines of isodoses [17].

2.3 Data Analysis

The results of particle tracking were obtained in ROOT file format [18], then the data, i.e. photon identifier number, type of interaction, position of interaction, and energy transferred were extracted for further analysis. In addition, two 3D matrices (0.1 mm resolution) storing the energy transferred and the related absorbed dose in the whole mouse were provided in two files in Analyze format [8, 19].

For each VOI, the relative importance for elementary interactions (Compton and photoelectric), the energy spectra, the total transferred energy and its related absorbed dose were also calculated.

3 Results

The energy transfer and dose were assessed with the 7 X-rays beams for each of the 7 energies. The total energy transferred in the 10 VOIs and for each of the 7 beam energies are reported in Table 1. Although low energy photons are more prone to transfer energy such as 50 keV in comparison to those at 450 keV (Table 1), the absorbed dose appeared high at higher energies (450 keV) than at lower energies (Table 2). Note the heart (V4 and V5) and the spine (V7 and V8) were not traversed by the beams although at some energies they received high doses. The regions V9 and V10 which included V1 also showed higher energy deposit.

Table 1. Total energy transferred in the 10 VOIs and for the 7 beam energies. Values for the tumor volume V1 are in MeV and the other VOIs have % values of those of V1 respectively for each beam energy.

	Beam energy (keV)						
VOIs	50	100	150	200	250	350	450
V1	6211	9947	17010	24810	32781	48656	63812
V2	0.64	0.27	0.18	0.15	0.12	0.1	0.08
V3	10.27	9.58	9.21	9.03	9.18	9.17	9.14
V4	1.14	1.03	0.47	0.28	0.16	0.1	0.07
V5	3.54	4.68	2.13	1.16	0.64	0.34	0.23
V6	0.95	0.51	0.35	0.3	0.26	0.22	0.18
V7	5.96	7.08	3.1	1.65	0.92	0.48	0.3
V8	0.1	0.09	0.05	0.04	0.03	0.02	0.02
V9	115.7	115.39	115.48	115.32	115.42	115.34	115.4
V10	128.85	129.33	129.43	129.27	129.39	129.3	129.5

Table 2. Absorbed dose in Gray in the 10 VOIs and for the 7 beam energies. The dose in V2 to V10 are % of their respective in V1 for a beam energy.

	Beam energy (keV)						
VOIs	50	100	150	200	250	350	450
V1	0.9123	1.4391	2.4430	3.5582	4.6796	6.8127	8.5674
V2	0	0	0	0	0	0	0
V3	0.11	0.11	0.1	0.1	0.1	0.1	0.11
V4	0.76	0.31	0.24	0.23	0.22	0.22	0.23
V5	0.06	0.04	0.03	0.03	0.03	0.03	0.03
V6	0.01	0.01	0	0	0	0	0.01
V7	6.6	2.89	0.97	0.45	0.27	0.15	0.12
V8	0.02	0.02	0.01	0.01	0	0	0
V9	1.4	1.39	1.4	1.39	1.39	1.37	1.35
V10	1.85	1.85	1.86	1.84	1.83	1.79	1.76

4 Discussion

MCS in small animal radiotherapy are accessible and handy tools to help for better designing treatment planning, not only to the target tumors and to the tissues along the beam paths, but also to distant organs of interest. It has been reported that doses of more than 5 Gy could be considered as lethal in mice [20, 21]. It is recognized that exposure to repeated radiations during follow-up studies can have biological effects on the animal models and thus can affect the experimental results. MCS can therefore help in designing the appropriate radiation energies, beam directions and intensity and duration of experiment. It is preferable to study each beam direction separately in order to determine its optimal parameters. Instead of using monoenergetic photons in the simulations, an energy spectrum resembling the one produced by an X-ray tube can be generated reproducing also its shape and intensity.

The radiation beams used in this simulation were based on X-rays tube voltage and current of 120 kVp and 50 mAs. The doses obtained in these simulations at lower energy (50 – 100 keV) were in the same range as those for micro-CT/radiotherapy or for radiotherapy previous studies at an effective energy around 50 keV (up to 2 Gy) [15, 16, 22, 23].

The variation of the dose in the heart and spine regions was a function of the beam energy, except for the 100 keV beam. Moreover, the volumes determined within the spinal cord received around 1% of the absorbed dose in the tumor, knowing that this volume was not on the path of any beam, and it was surrounded by bones. The spinal bones, however, and including the spinal cord, received higher doses with respect to spinal cord and heart VOIs. In fact, V7 received 6.6 times the dose of the tumor at 50 keV and 0.12 at 450 keV. This high ratio at 50 keV could be due to the high scattering in the mouse at this energy and high attenuation in the bones. The high doses calculated in V9 and V10 and in V1 at energies above 150 keV were due to the high number of generated photons. In real treatments, the number of photons is also governed by beam application duration among other parameters.

The two extra volumes around the lung tumor directly received the beam from some angles, but they were not directly exposed to the beams for some other beam angles. Also, the tissue density of these extra volumes was less than that of the tumor. Despite these differences, photons interactions in these volumes V9 and V10 varied very slightly with beam energies in comparison to V1, and their average ratios of absorbed dose (average over beam energies) were $V9/V1 = 1.3841 \pm 0.0194$ Gy and $V10/V1 = 1.8265 \pm 0.0372$ Gy. Apart from uncertainty on tumor volume definition, the X-rays focal spot on the anode could also cause a penumbra that can have an impact on tumor neighboring tissues [15, 16].

5 Conclusions

The goal of this study was to assess the photon energy transfer and absorbed dose in tissues distant from or partially intercepted by the radiation beams as a function of beam energy. The spinal cord, even protected by the spinal bones and not intercepted by the beams, received in average 1% of the dose to the tumor, which, in turn, received 0.9 Gy at 50 keV and 8.56 Gy at 450 keV. The lowest dose to the secondary organs was found at the 100 keV beam. The dose to tumor surrounding tissue was shown to be independent of beam energy and had ratios of 1.38 and 1.83 for volumes of diameters 1.6 mm and 1.8 mm with respect to the lung tumor of diameter 1.4 mm.

Acknowledgements. The authors wish to thank M. HuiZhong Lu for his kind assistance in software installation on the supercomputer Mammouth at Université de Sherbrooke.

Computations were made on the supercomputer Mammouth MS2, Université de Sherbrooke, managed by Calcul Québec and Compute Canada. The operation of this supercomputer is funded by the Canada Foundation for Innovation (CFI), Nano-Québec, RMGA and the Fonds de recherche du Québec - Nature et technologies (FRQ-NT).

Conflict of interest disclosure. the authors declare that they have no conflict of interest.

References

1. Leal, A., Sanchez-Doblado, F., Perucha, M., Carrasco, E., Rincon, M., Arrans, R., Bernal, C.: Monte Carlo Simulation of Complex Radiotherapy Treatments. Computing in Science and Engg. 6(4), 60–68 (2004)
2. Wang, H., Ma, Y., Pratx, G., Xing, L.: Toward Real-Time Monte Carlo Simulation Using a Commercial Cloud Computing Infrastructure. Physics in Medicine and Biology 56(17), N175–N181 (2011)
3. Dogdas, B., Stout, D., Chatziioannou, A.F., Leahy, R.M.: Digimouse: a 3D whole body mouse atlas from CT and cryosection data. Phys. Med. Biol. 52(3), 577–587 (2007)
4. Segars, W.P., Tsui, B.M.W.: MCAT to XCAT: The Evolution of 4-D Computerized Phantoms for Imaging Research. Proceedings of the IEEE 97(12), 1954–1968 (2009)

5. Mauxion, T., Barbet, J., Suhard, J., Pouget, J.-P., Poirot, M., Bardiès, M.: Improved realism of hybrid mouse models not be sufficient to generate reference dosimetric data. Medical Physics 40(5), 052501 (2013)
6. Jan, S., Santin, G., Strul, D., Staelens, S., Assié, K., Autret, D., Avner, S., Barbier, R., Bardiès, M., Bloomfield, P.M., Brasse, D., Breton, V., Bruyndonckx, P., Buvat, I., Chatziioannou, A.F., Choi, Y., Chung, Y.H., Comtat, C., Donnarieix, D., Ferrer, L., Glick, S.J., Groiselle, C.J., Guez, D., Honore, P., Kerhoas-Cavata, S., Kirov, A.S., Kohli, V., Koole, M., Krieguer, M., van der Laan, D.J., Lamare, F., Largeron, G., Lartizien, C., Lazaro, D., Maas, M.C., Maigne, L., Mayet, F., Melot, F., Merheb, C., Pennacchio, E., Perez, J., Pietrzyk, U., Rannou, F.R., Rey, M., Schaart, D.R., Schmidtlein, C.R., Simon, L., Song, T.Y., Vieira, J., Visvikis, D., Van de Walle, R., Wieërs, E., Morel, C.: GATE - Geant4 Application for Tomographic Emission: a simulation toolkit for PET and SPECT. Phys. Med. Biol. 49(19), 4543–4561 (2004)
7. Schneider, W., Bortfeld, T., Schlegel, W.: Correlation between CT numbers and tissue parameters needed for Monte Carlo simulations of clinical dose distributions. Phys. Med. Biol. 45(2), 459–478 (2000)
8. Sarrut, D., Bardies, M., Boussion, N., Freud, N., Jan, S., Letang, J.M., Loudos, G., Maigne, L., Marcatili, S., Mauxion, T., Papadimitroulas, P., Perrot, Y., Pietrzyk, U., Robert, C., Schaart, D.R., Visvikis, D., Buvat, I.: A review of the use and potential of the GATE Monte Carlo simulation code for radiation therapy and dosimetry applications. Med. Phys. 41(6), 064301 (2014)
9. Chow, J.C.L., Leung, M.K.K.: Treatment planning for a small animal using Monte Carlo simulation. Medical Physics 34(12), 4810–4817 (2007)
10. Mah, P., Reeves, T.E., McDavid, W.D.: Deriving Hounsfield units using grey levels in cone beam computed tomography. Dentomaxillofac Radiol. 39(6), 323–335 (2010)
11. Suryanto, A., Herlambang, K., Rachmatullah, P.: Comparison of tumor density by CT scan based on histologic type in lung cancer patients. Acta Med. Indones 37(4), 195–198 (2005)
12. Larsson, E., Ljungberg, M., Strand, S.-E., Jönsson, B.-A.: Monte Carlo calculations of absorbed doses in tumours using a modified MOBY mouse phantom for pre-clinical dosimetry studies. Acta Oncologica 50(6), 973–980 (2011)
13. Loening, A.M., Gambhir, S.S.: AMIDE: a free software tool for multimodality medical image analysis. Mol. Imaging 2(3), 131–137 (2003)
14. Kirkpatrick, J.P., van der Kogel, A.J., Schultheiss, T.E.: Radiation Dose–Volume Effects in the Spinal Cord. International Journal of Radiation Oncology*Biology*Physics 76(suppl. 3), S42–S49 (2010)
15. Rodriguez, M., Zhou, H., Keall, P., Graves, E.: Commissioning of a novel microCT/RT system for small animal conformal radiotherapy. Phys. Med. Biol. 54(12), 3727–3740 (2009)
16. Zhou, H., Rodriguez, M., van den Haak, F., Nelson, G., Jogani, R., Xu, J., Zhu, X., Xian, Y., Tran, P.T., Felsher, D.W., Keall, P.J., Graves, E.E.: Development of a MicroCT-Based Image-Guided Conformal Radiotherapy System for Small Animals. Int. J. Radiat. Oncol. Biol. Phys. 78(1), 297–305 (2010)
17. Chow, J.C.L.: Dosimetric impact of monoenergetic photon beams in the small-animal irradiation with inhomogeneities: A Monte Carlo evaluation. Radiation Physics and Chemistry 86(0), 31–36 (2013)
18. Brun, R., Rademakers, F.: ROOT — An object oriented data analysis framework. Nuclear Instruments and Methods in Physics Research Section A: Accelerators, Spectrometers, Detectors and Associated Equipment 389(1-2), 81–86 (1997)

19. Visvikis, D., Bardies, M., Chiavassa, S., Danford, C., Kirov, A., Lamare, F., Maigne, L., Staelens, S., Taschereau, R.: Use of the GATE Monte Carlo package for dosimetry applications. Nuclear Instruments and Methods in Physics Research Section A: Accelerators, Spectrometers, Detectors and Associated Equipment 569(2), 335–340 (2006)
20. Ford, N.L., Thornton, M.M., Holdsworth, D.W.: Fundamental image quality limits for microcomputed tomography in small animals. Med. Phys. 30(11), 2869–2877 (2003)
21. Bartling, S.H.: Small Animal Computed Tomography Imaging. Current Medical Imaging Reviews 3, 45–59 (2007)
22. Taschereau, R., Chow, P.L., Chatziioannou, A.F.: Monte Carlo simulations of dose from microCT imaging procedures in a realistic mouse phantom. Med. Phys. 33(1), 216–224 (2006)
23. Graves, E.E., Zhou, H., Chatterjee, R., Keall, P.J., Gambhir, S.S., Contag, C.H., Boyer, A.L.: Design and evaluation of a variable aperture collimator for conformal radiotherapy of small animals using a microCT scanner. Medical Physics 34(11), 4359–4367 (2007)